Analytica Chimica Acta 776 (2013) 17–23

Contents lists available at SciVerse ScienceDirect

Analytica Chimica Acta

journal homepage: www.elsevier.com/locate/aca

Fabrication of glucose biosensor for whole blood based on Au/hyperbranched polyester nanoparticles multilayers by antibiofouling and self-assembly technique

Chong Sun[a,b,1], Xiaohan Chen[a,1], Qiaorong Han[a], Min Zhou[c], Chun Mao[a,*], Qinshu Zhu[a], Jian Shen[a,*]

[a] Jiangsu Key Laboratory of Biofunctional Materials, College of Chemistry and Materials Science, Nanjing Normal University, Nanjing 210023, China
[b] Key Laboratory for Soft Chemistry and Functional Materials of Ministry of Education, School of Chemical Engineering, Nanjing University of Science and Technology, Nanjing 210094, China
[c] Department of Vascular Surgery, the Affiliated Drum Tower Hospital of Nanjing University Medical School, Nanjing 210008, China

HIGHLIGHTS

- A novel method for detection of glucose in whole blood has been developed.
- The method based on antibiofouling and self-assembly technology was investigated.
- The antibiofouling technique utilized for sensor is significant for diagnostics.

GRAPHICAL ABSTRACT

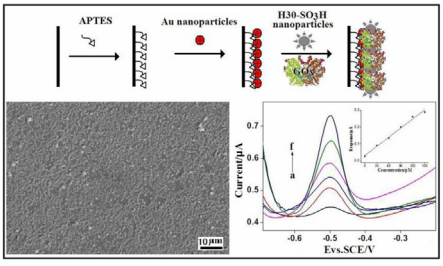

ARTICLE INFO

Article history:
Received 22 January 2013
Received in revised form 7 March 2013
Accepted 12 March 2013
Available online 21 March 2013

Keywords:
Hyperbranched polyester nanoparticles
Antibiofouling
Self-assembly technology
Glucose nano-biosensors
Whole blood

ABSTRACT

Acknowledging the benefits of hyperbranched polymers and their nanoparticles, herein we report the design and synthesis of sulfonic acid group functionalized hydroxyl-terminated hyperbranched polyester (H30-SO_3H) nanoparticles and their biomedical application. The H30-SO_3H nanoparticles were characterized by transmission electron microscopy (TEM), Fourier transform infrared (FTIR) spectroscopy and proton nuclear magnetic resonance spectroscopy (^{1}H NMR). The good hemocompatibility of H30-SO_3H nanoparticles was also investigated by coagulation tests, complement activation and platelet activation. The novel glucose biosensor was fabricated by immobilizing the positively charged Au nanoparticles, H30-SO_3H nanoparticles and glucose oxidase (GOx) onto the surface of glassy carbon electrode (GCE). It can be applied in whole blood directly, which was based on the good hemocompatibility and antibiofouling property of H30-SO_3H nanoparticles. The biosensor had good electrocatalytic activity toward glucose with a wide linear range (0.2–20 mM), a low detection limit 1.2×10^{-5} M in whole blood and good anti-interference property. The development of materials science will offer a novel platform for application to substance detection in whole blood.

1. Introduction

The clinical conditions of diabetes mellitus are well known and well understood, yet remain a growing concern as the prevalence of the disease increases worldwide at an alarming rate [1]. Accurate blood glucose values play an especially important role in the diagnosis of diabetes. In principle, blood glucose values should be given

* Corresponding authors. Tel.: +86 25 85891635; fax: +86 25 83598280.
E-mail addresses: maochun127@yahoo.cn (C. Mao), jshen@njnu.edu.cn (J. Shen).
[1] These authors made equal contribution to this paper.

0003-2670/$ – see front matter © 2013 Elsevier B.V. All rights reserved.
http://dx.doi.org/10.1016/j.aca.2013.03.032

in terms of whole blood, but most hospitals and laboratories now measure and report the serum glucose levels. There are two major reasons for this situation. On one hand, the red blood cells have a higher concentration of protein (e.g. hemoglobin) than serum. On the other hand, serum has a higher water content, therefore, more dissolved glucose than it does in whole blood. To convert from whole-blood glucose, multiplication by 1.15 has been shown to generally give the serum/plasma level [2]. However, the test results are influenced by the different model numbers of test instruments and detection reagents, treatment processes of blood samples, factitious operations, especially additional centrifuge and too long measure time from collecting specimen of blood to examination. Meanwhile, it is very difficult to design and prepare a electrochemical biosensor that can be used in whole blood just because the biofouling of electrode surface can be developed by platelet, fibrin and blood cell adhesion in the complex environment of whole blood media. And the biofouling of electrode surface will bring catastrophic damage to the electron transfer between enzyme and electrode redox center.

The use of home glucose meters for the diagnosis of diabetes is not recommended because of their potential for imprecision. Moreover, the blood samples are obtained from fingertip peripheral but not vein, and doped easily with tissue fluid.

The development of nanomaterials for the ultra sensitive detection of biological species has received great attention because of their unique optical, electronic, chemical and mechanical properties. Most studies focus on metal (gold, silver), carbon and conducting polymers that used to prepare nanomaterials such as nanoparticles [3,4], nanotubes [5,6] and nanowires [7–9]. Analysts in this field are always enthusiastic about finding new materials with good biocompatibility to improve the behavior of biosensors [10,11]. Despite many technological advances in biosensor research and development and the introduction of many different products, glucose biosensors were still performed in serum [12–16]. The focus of this paper is the development and investigation of antibiofouling properties of new nanostructured architecture for electrochemical glucose biosensors that applied in whole blood directly. The strategy for decorating electrode of glucose biosensor with Au/hyperbranched polyester nanoparticles multilayers that exhibit excellent antibiofouling property was suggested. This robust strategy demonstrates a methodology for the incorporation of actively antibiofouling moieties onto a passively antibiofouling electrode, and thus expands the range of applications of electrochemical glucose biosensors. The fundamental nature of interpenetration of nanotechnology, antibiofouling, and biosensor technology was investigated.

2. Experimental

2.1. Materials

H30 (Third-generation aliphatic hyperbranched polyester with 24 terminal hydroxyl groups) was obtained from Suzhou HyperT Resin Science & Technology Co. Ltd. and used with further precipitation and purification. Hydrogen tetrachloroaurate (β) trihydrate ($HAuCl_4{\cdot}3H_2O$, 99.9%) was obtained from Alfa Aesar, a Johnson Matthey Company. Glucose oxidase (GOx), ascorbic acid (AA) and uric acid (UA) were obtained from Sigma–Aldrich Co., β-D-(+)-glucose (99%) was from J&K Chemical Co. Inc. Dimethylsulfoxide (DMSO), tetrahydrofuran (THF), sodium hydride, 1,3-propane sultone, tetraoctylammonium bromide, toluene, $NaBH_4$ and 4-dimethylaminopyridine (DMAP) were purchased from Sinopharm Chemical reagent Co. Ltd. THF was dried by refluxing over sodium and distilled just prior to use. Other reagents were used without further purification. All solutions were prepared with double-distilled water and all chemicals and solvents were of analytical grade.

2.2. Instrumentation

Transmission electron microscopy (TEM) images were obtained by using an interface high-resolution transmission electron microscopy (HITACHI H-7650, Japan). The FTIR spectra of H30 and H30-SO_3H nanoparticles were measured using a Cary 5000 Fourier transform infrared spectrophotometer (VARIAN Cary 5000, USA). Proton nuclear magnetic resonance spectroscopy (^{1}H NMR) experiments were performed by using a Bruker Avance 400 spectrometers (Bruker, Germany).

2.3. Procedures

2.3.1. Functionalization of H30 with sulfonic acid groups (H30-SO_3H)

The preparation of H30-SO3H nanoparticles was prepared by a procedure described in the previous references [17,18]. In brief, the hyperbranched polyester H30 (1.0 g, with 9.06 mM of —OH groups) was dissolved in THF in a three-necked round-bottomed flask equipped with a magnetic stirrer and a reflux condenser with a drying tube. Excess sodium hydride (0.76 g), corresponding to the theoretical quantity of hydroxy groups of the polyester H30, was then dissolved in THF and added to the polymer solution. The reaction mixtures were reacted at 70 °C for 12 h with stirring before adding 1,3-propane sultone (1.66 g) and then allowed to react at 70 °C last longer than 12 h. The resulting product was filtered and dissolved in DMSO, then precipitated in acetone and dried in vacuum oven. The crude product was purified by dialysis through dialysis bag (MWCO 500) for at least five days. After dialysis, the solution was dried under vacuum and a white product H30-SO_3H was obtained.

2.3.2. Synthesis of the positively charged Au nanoparticles

The positively charged Au nanoparticles were prepared by a spontaneous phase transfer method [19,20] but with a slight variation. Typically, a 30 mM aqueous $HAuCl_4{\cdot}3H_2O$ solution (30 mL) was added to a 25 mM solution of tetraoctylammonium bromide in toluene (80 mL). The transfer of the metal salt to the toluene phase could be clearly seen visually within a few seconds. A 0.4 M solution of freshly prepared $NaBH_4$ (25 mL) was added to the stirred mixture, which caused an immediate reduction to occur. After 30 min the two phases were separated and the toluene phase was subsequently washed with 0.1 M H_2SO_4, 0.1 M NaOH, and H_2O (three times), and then dried over anhydrous Na_2SO_4. Then an aqueous 0.1 M DMAP solution was added to the nanoparticle mixtures. Direct phase transfer across the organic/aqueous boundary was completed within 1 h, with no stirring or agitation required.

2.3.3. Hemocompatibility of H30-SO_3H nanoparticles

The *in vitro* blood compatibility evaluated H30-SO_3H nanoparticles by coagulation tests, complement activation and platelet activation. The experimental procedure to evaluate the hemocompatibility of nanoparticles was described in our previous report [21–23]. Briefly, activated partial thromboplastin time (APTT), prothrombin time (PT), and thromboplastin time (TT) of the H30-SO_3H nanoparticles were measured on a semi automated coagulometer (RT-2204C, Rayto, USA). The blood was obtained from a healthy adult rabbit anticoagulated with sodium citrate solution. Plasma was prepared by centrifuging rabbit blood at 2500 rpm for 15 min and then used for testing. Plasma was mixed with the H30-SO_3H nanoparticles, for a contact time of 3 min. Each sample was measured three times to give an average value.

Hemocompatibility of the H30-SO_3H nanoparticles was also evaluated by measuring complement and platelet activation under *in vitro* conditions. The complement system is a primary

contributor to the innate immune system of the host, clearing the body of foreign cells and organisms through direct lysis or by recruiting leukocytes that promote phagocytosis [24,25]. *In vitro* plasma coagulation tests are of low value due to their low sensitivity and the presence of strong external initiators of coagulation (neoplastin reagent, calcium, thrombin). Thus only dramatic changes can be detected, while weaker physiologically relevant effects could be masked by the excess of the external coagulation initiators. To assess the complement activation, the cleavage of complement component C3 was monitored by measuring the formation of its activation peptides, C3a and C3a des-Arg, using a commercial C3a enzyme immunoassay kit with a flow cytometer (FACSCalibur; BD Biosciences, USA) according to the manufacturer's instructions. Activation studies were performed on platelet poor plasma (PPP) isolated by centrifugation from human whole blood donations. The plasma and the H30-SO_3H nanoparticles with required concentration in saline were incubated at 37 °C for 1 h. All the complement activation experiments were done in triplicates.

To measure the platelet activation, the platelet rich plasma (PRP) was incubated at 37 °C with a required concentration of the H30-SO_3H nanoparticles suspension. The incubation mixture was removed at 30 min to assess the activation state of the platelets using fluorescence flow cytometry. Expression of the fluorescently labeled platelet activation marker anti-CD62P and the platelet pan-marker anti-CD42a were detected by using a BD FACSCalibur and a double staining method according to the manufacturer's instructions. All the platelet activation experiments were done in triplicates.

2.3.4. Characterization of GOx-(H30-SO_3H)/Au hybrids

The circular dichroism (CD) spectra were taken using a JASCO J-715 spectropolarimeter. Quartz cells of 1 cm optical path length were used for all CD measurements of GOx (GOx concentration = 0.06 mg mL^{-1}) and GOx/(H30-SO_3H)/Au (GOx: (H30-SO_3H)/Au = 1:1 weight ratio) solutions. The phosphate buffer (Na_2HPO_4–NaH_2PO_4, pH 7.4) was used to prepare these solutions. The spectra were analyzed for the content of secondary structure by using the JASCO710 program accompanying the spectropolarimeter.

2.3.5. Construction of GOx-(H30-SO_3H)/Au/APTES/GCE and measurements

Prior to the modification, the GCE was successively polished to a mirror-like surface with 0.3 and 0.05 μm alumina slurry followed by rinsing thoroughly with double-distilled water. After being sonicated in ethanol and double-distilled water for 5 min, respectively, the GCE was allowed to dry at room temperature.

As shown in Scheme 1, 8.0 μL of 0.1% (3-aminopropyl) triethoxysilane (APTES) solution (anhydrous alcohol as solvent) was successively dropped onto the electrode surface and dried in air. APTES was linked to the GCE surface through the silicon–oxygen bonds. The pretreated GCE was cast with 8.0 μL positively charged Au nanoparticles aqueous and dried in room temperature. After that, the Au nanoparticles were combined with the amino at the end of APTES molecule. Finally, the fresh prepared mix solution of 4.0 μL 6 mg mL^{-1} GOx solution and 4.0 μL 1 mg mL^{-1} H30-SO_3H nanoparticles aqueous was dropped onto the surface of Au/APTES/GCE and kept overnight at 4 °C. Thus, the GOx and the H30-SO_3H nanoparticles were immobilized by electrostatic absorption, and GOx-(H30-SO_3H)/Au/APTES/GCE was obtained. The other electrodes used as contrast samples were prepared by the same modified method. When not in use, the electrodes were stored at 4 °C in a refrigerator.

The antibiofouling property of the H30-SO_3H nanoparticles modified GCE was evaluated by whole blood adhesion test under *in vitro* conditions. The blank GCE substrate without H30-SO_3H nanoparticles and GOx/(H30-SO_3H) modified GCE were cast on the 24-well microplates and immersed in PBS for 24 h. The disks were immersed in whole blood at 37 °C for 1 h and then transferred to a saline solution containing 2.5% glutaraldehyde to immobilize the bounded blood cells. The disks were rinsed, air-dried, coated with gold, and then the surface was investigated by scanning electron microscopy (SEM, JEOL JSM Model 6300, Japan).

Cyclic voltammetry studies used a CHI 760D electrochemical workstation (Shanghai Chenhua Apparatus Corporation, China). All experiments were carried out using a three-electrode cells equipped with a Pt-wire as counter electrode and a saturated calomel electrode (SCE) as reference electrode. The applied scan rate was 100 mV s^{-1}.

Amperometric measurements were conducted in a 5 mL PBS cell at room temperature and the solution was purged with high purity nitrogen firstly and blanked with nitrogen during the electrochemical experiments. The electrochemical impedance spectroscopy (EIS) tests were carried out in the frequency range of 1 Hz–100 kHz with a 5 mV AC amplitude. The data points were taken after 2 s quiet time (12 data points per frequency decade). Differential pulse voltammetry (DPV) measurements were carried out with pulse amplitude of 0.05 V and pulse width of 0.2 s. Different concentrations of glucose solution were added under intensive stirring, then cyclic voltammogram (CV) was performed until the currents did not change any more, and DPV was immediately carried out. Then correlation between response currents and different concentrations of glucose solution was obtained.

The anti-interference property of biosensor was carried out by adding 0.1 mM glucose, followed by 10 mM AA, 10 mM UA and 0.1 mM glucose. Blood samples were obtained from various volunteers, within sodium fluoride to prevent glucose metabolism by blood cells prior to glucose determination [26]. Real sample analysis of the biosensor was compared with hospital biochemistry laboratory.

3. Results and discussion

3.1. Characterization of H30-SO_3H nanoparticles

Hyperbranched polymers composed of densely branched structures adopt compact conformations with a large number of surface reactive groups. The structural formula of the H30-SO_3H

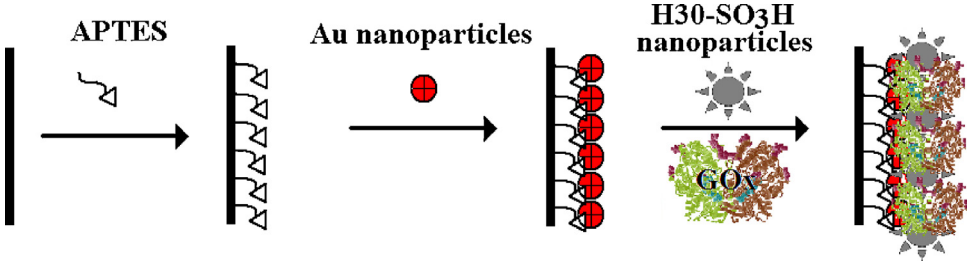

Scheme 1. The process of the GOx-(H30-SO_3H)/Au/APTES modified electrode.

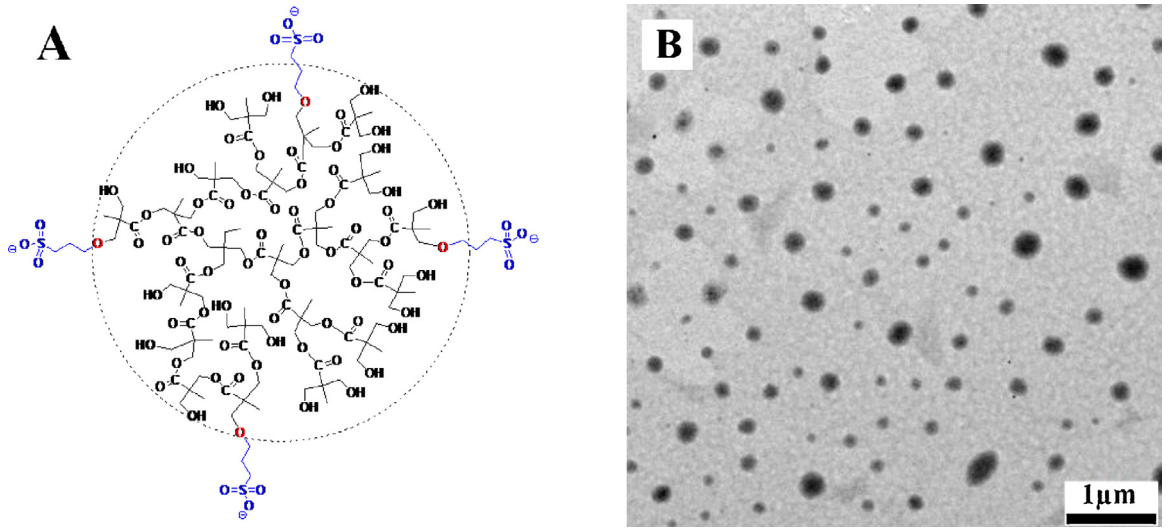

Fig. 1. (A) The chemical structure of H30-SO_3H nanoparticles, and (B) TEM images of H30-SO_3H nanoparticles.

nanoparticle was shown in Fig. 1(A). As shown in Fig. 1(B), the H30-SO_3H nanoparticles were formed. TEM photograph of the nanoparticles showed the average diameter of 210 nm. FTIR spectra of H30 and H30-SO_3H nanoparticles were represented in Fig. S1(A). The spectra for H30-SO_3H nanoparticles have vibration bands at 1195 and 1045 cm^{-1}, which are identified as O=S=O symmetric stretching and SO_3^- stretching modes in SO_3H, respectively [27]. The results indicated that H30-SO_3H nanoparticles were synthesized based on a hyperbranched polyester with hydroxyl terminal-groups by modifying with sulfonic acid groups. The ^1H NMR spectrum of H30-SO_3H with SA_{arm} = 4 was shown in Fig. S1(B). Comparing the ^1H NMR spectra of H30-SO_3H with that of H30, new proton signals appeared at 3.14–3.43, 2.46–2.53, 1.68–1.89 ppm (protons h, i and j), which confirmed that 1,3-propane sultone was grafted successfully through the formation of ester bondings. The conversion ratio from hydroxyl groups to sulfonic acid groups could be calculated by comparing the integral of peaks f and g with the integral of peaks a and c ($1–11S_{f,g}/2S_{a,c}$) is about 17.48%.

3.2. Hemocompatibility of H30-SO_3H nanoparticles

The good hemocompatibility of H30-SO_3H nanoparticles was investigated by coagulation tests, complement activation and platelet activation. More detailed explanations were presented in Supplementary Material.

The whole blood adhesion test has already become a recognized technique to estimate the blood compatibility or anticoagulation of a prepared material surface. Fig. 2 shows SEM pictures of the surface coated with and without GOx/(H30-SO_3H) after contact with whole blood. Platelet deposition and blood cells were observed on the surface of blank GCE (Fig. 2(A)). In the case of the GCE's surface modified with H30-SO_3H nanoparticles, platelet deposition and blood cell adhesion were suppressed on the surface (Fig. 2(B) and (C)). The results strongly indicated that thrombus were difficult to form onto the surface of GOx/(H30-SO_3H) without fused blood cells and platelets. The antibiofouling effect of H30-SO_3H nanoparticles could efficiently suppress blood-cell adhesion and create a good microenvironment for GOx to undergo facile electron-transfer reactions.

3.3. Characterization of GOx-(H30-SO_3H)/Au hybrids

Recently, CD has been widely used to analyze the main properties and features of enzyme solutions and films [28]. The most utilized form of CD spectroscopy is far-UV CD (190–260 nm), which is analyzed to estimate the secondary structure content of the proteins due to its correspondence to electronic transitions of the backbone chromophore of the enzyme [29]. At present, CD spectra were used to characterize the secondary structure of GOx after it hybrided with (H30-SO_3H)/Au. Fig. S3 displays the CD spectra of GOx and GOx-(H30-SO_3H)/Au hybrids. Spectral analysis could provide estimates of the secondary structure content, and the results of such analysis were presented. The contents of α-helix and β-turn conformation of GOx-(H30-SO_3H)/Au changed by 2.8% and 0.3% compared with pure GOx. Indeed, it could be seen that the CD spectrum of GOx-(H30-SO_3H)/Au bioconjugates looks similar to the pure GOx, but the peak had slightly more intensity. It indicated that the GOx had been adsorbed on the surface of (H30-SO_3H)/Au. In fact, the similar secondary structure content of GOx and GOx-(H30-SO_3H)/Au indicated that the secondary structure of GOx was preserved after hybriding with (H30-SO_3H)/Au [30].

3.4. Direct electron transfer reactivity and calibration curve

The electrochemical behavior of the GOx-(H30-SO_3H)/Au/APTES/GCE was investigated by amperometric methods. Cyclic voltammetry is a valuable tool for testing the kinetic barrier of the interface. The electron transfer between a solution species and the electrode must occur by tunneling either through the barrier or through the defects in the barrier [31,32]. Therefore, it is chosen as a marker to investigate the changes of electrode behavior after each assembly step [33]. Fig. 3(A) shows CVs of differently modified electrodes in 0.1 M PBS (pH = 7.4) at a scan rate of 100 mV s^{-1}. No voltammetric signal was observed at APTES/GCE (curve a) and Au/APTES/GCE (curve b) in the range of −1.0 to 0.2 V. When GOx was embedded in the Au/APTES/GCE, the obtained CV curve was almost flat (curve c). When GOx was embedded in the H30-SO_3H nanoparticles, there was just a pair of little parcels that could be observed (curve d). The two little parcels were oxidation-reduction peaks of GOx. The small peaks mean that electron transfer of GOx on (H30-SO_3H)/GCE was very slow. However, only when the matrix that containing GOx and H30-SO_3H nanoparticles were embedded in Au/APTES/GCE (curve e), could a pair of well-defined oxidation and reduction peaks be observed with a formal potential ($E^{\circ\prime}$) at about −0.461 V. These results further demonstrate that the integrated structure of GOx molecule remains unchangeable after the immobilization on the GCE, which is in good agreement with that obtained from spectroscopic results. Meanwhile, the positively charged Au

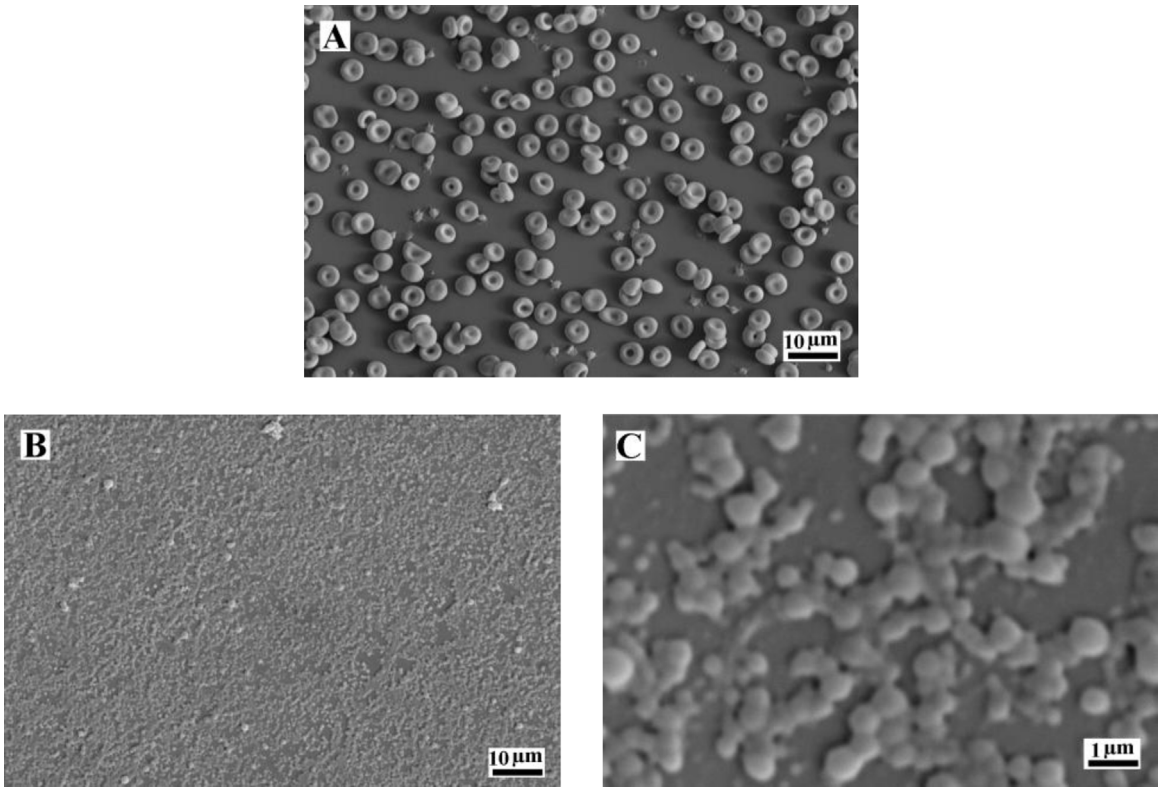

Fig. 2. SEM images of (A) blank GCE substrate, (B) GCE substrate modified with GOx/(H30-SO_3H), and (C) enlarge view from (B) exposed to human whole blood for 60 min, respectively.

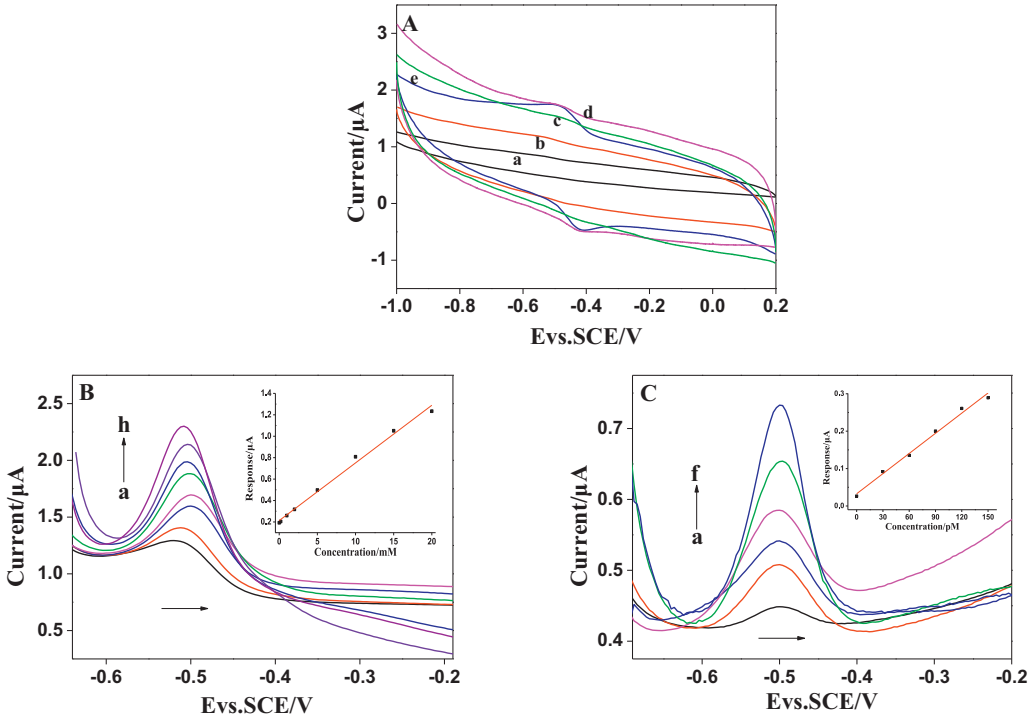

Fig. 3. (A) CV of (a) APTES/GCE, (b) Au/APTES/GCE, (c) GOx/Au/APTES/GCE, (d) GOx/(H30-SO_3H)/APTES/GCE, and (e) GOx-(H30-SO_3H)/Au/APTES/GCE in 0.1 M PBS (pH = 7.4). Scan rate: 100 mV s^{-1}. (B) DPVs obtained at GOx-(H30-SO_3H)/Au/APTES/GCE in 0.1 M PBS (pH = 7.4) with the concentration of glucose (from a to g) 0, 0.2, 1, 2, 5, 10, 15, 20 mM; and the insert: relationship between the peak current and the concentration of glucose. (C) DPVs obtained at GOx-(H30-SO_3H)/Au/APTES/GCE in whole blood samples at 25 °C with glucose of (a) 0 pM, (b) 30 pM, (c) 60 pM, (d) 90 pM, (e) 120 pM, (f) 150 pM; and the insert: relationship between the peak current and the concentration of glucose in whole blood samples. The horizontal arrow in (B) and (C) indicated the scan direction.

Table 1
Comparison of the responses of some glucose biosensors constructed based on different modified electrode materials that reported by previous papers.

Electrode materials	Linear range (mM)	Detection limit (mM)	Correlation coefficient	Ref.
Poly(pyrrole propylic acid)/Au	1–18	0.05	0.998	[34]
Au nanoparticle-CS composite film	0.4–10.7	0.37	0.999	[35]
Nafion-GOx-OMC	0.5–1.5	0.157	0.995	[36]
GOx-graphene-chitosan	0.08–12	0.02	0.999	[37]
GOx-graphene-AuNPs-chitosan	2–10	0.18	0.991	[38]
GOx-(H30-SO_3H)/Au	0.2–20	0.012	0.996	This work

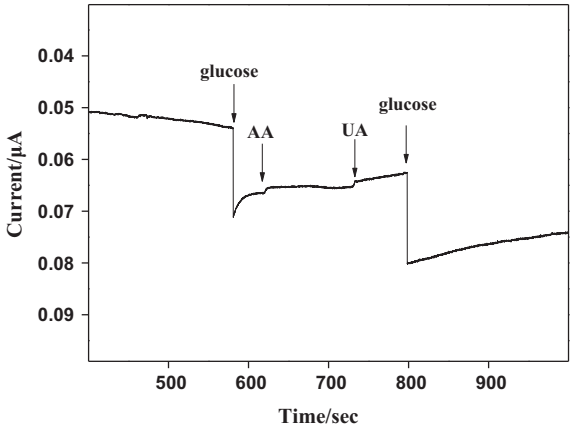

Fig. 4. Amperometric responses of the biosensor upon additions of glucose (0.1 mM), AA (10 mM), and UA (10 mM), in PBS. The biosensor was biased on the potential of −0.46 V.

nanoparticles and the negatively charged H30-SO_3H nanoparticles play important roles in facilitating the electron exchange between the electroactive center of GOx and GCE.

Fig. 4 exhibits the electrochemical impedance spectra of the electrode surface status. More detailed explanations were presented in Supplementary Material.

A series of DPVs were recorded at various concentrations of glucose to determine its calibration curve in PBS and whole blood. Moderate stirring was kept for about 1 min when glucose solution was successively added to the buffer solution prior to recording the DPV voltammograms. The linear response range was obtained from 0.2 to 20 mM and the linear regression equation was I (μA) = 0.053c (mM) + 0.212 (R = 0.9964), where I was current and c was the glucose concentration (Fig. 3(B)). The enhanced linear range expands the applications of the biosensor, especially in the glucose determination in whole blood samples. In this work, we also investigated the DPVs of the GOx-(H30-SO_3H)/Au/APTES/GCE in the detection of glucose in human whole blood. The current response was determined in 5 mL of 0.1 M, pH 7.4 PBS containing whole blood sample of 500 μL. The current response was recorded for glucose in varying concentrations in healthy human whole blood. The DPV curves in Fig. 3(C) show that the peak current gradually shifted to be positive with increasing concentrations of glucose and an anodic peak was observed at −0.48 V. The results clearly showed that the variation of the DPV peak current *vs.* glucose concentration was linear with a detection limit and correlation coefficient of 1.2×10^{-5} M (S/N = 3) in whole blood and 0.9956, respectively.

Moreover, an analytical performance comparison of some glucose biosensors reported by previous papers and the novel biosensor we prepared was performed. From Table 1, we can conclude that the proposed biosensor exhibited excellent performance in terms of a wider linear range and lower limit of detection for glucose [34–38]. The good performance implies that H30-SO_3H nanospheres can provide a good biocompatible microenvironment for maintaining enzymatic activity.

Table 2
Determination of glucose in whole blood samples using the GOx-(H30-SO_3H)/Au/APTES/GCE.

No.	Referenced values[a] (mM)	Determined values[b] (mM)
1	4.8 ± 0.21	4.7 ± 0.26
2	5.3 ± 0.17	5.0 ± 0.23
3	5.7 ± 0.15	5.5 ± 0.24
4	11.5 ± 0.31	11.2 ± 0.34
5	16.5 ± 0.19	16.3 ± 0.21

[a] Referenced values were provided by the hospital biochemistry laboratory.
[b] The values were determined by the GOx-(H30-SO_3H)/Au/APTES/GCE; they were average values of five measurements for each sample.

3.5. Effect of interferents analysis

An important analytical parameter for a biosensor is its ability to discriminate between the interfering species commonly present in similar physiological environment and the target analyte [39]. Electrochemical response of the GOx-(H30-SO_3H)/Au/APTES/GCE was examined in the presence of some electroactive interfering substances like AA and UA at higher levels than normal physiological [39]. The experiment was carried out by adding 0.1 mM glucose followed by 10 mM AA, 10 mM UA and 0.1 mM glucose. As shown in Fig. 4, the electroactive species did not cause interference significantly for the determination of glucose. These results imply that the GOx-(H30-SO_3H)/Au/APTES/GCE has a good anti-interference ability.

3.6. Real sample analysis

In order to verify the reliability of the biosensor, it was applied for the determination of glucose in whole blood samples. The blood samples and their glucose concentrations were provided by hospital biochemistry laboratory. The samples were then reassayed with the GOx-(H30-SO_3H)/Au/APTES/GCE. The results were agreed closely with those values measured in hospital (Table 2). Furthermore, compared with the values measured in serum samples which are isolated from whole blood by biochemical analyzer, the values we measured in whole blood directly by the GOx-(H30-SO_3H)/Au/APTES/GCE biosensor are more close to the real values probably. Thus, the biosensor can be used for the glucose detection in whole blood sample and further investigation will be done by our research group in near future.

4. Conclusion

Analysts are always enthusiastic about finding new materials with good biocompatibility to improve the behavior of biosensors. In this case, a novel electrochemical biosensor, which can be conveniently applied for accurate quantification of the level of blood glucose with the help of antibiofouling and self-assembly technology, was investigated. To the best of our knowledge, this is the first time that the hyperbranched polymer nanoparticles functionalized by sulfonic acid group have been utilized to prepare a novel biosensor suitable for glucose detection in whole blood directly. The integration of the technologies, which includes

anticoagulant, sensor and nanoscience, will bring significant input to high-performance biosensors relevant to diagnostics and therapy of interest for human health.

Acknowledgments

The work is supported by NSFC (21144002, 81201210), NSFJS (BK2011781), Major Program for the NSFRHEI of Jiangsu Province (12KJA150006), the Priority Academic Program Development of Jiangsu Higher Education Institutions, and Research project of Jiangsu Province (BY2011109).

Appendix A. Supplementary data

Supplementary data associated with this article can be found, in the online version, at http://dx.doi.org/10.1016/j.aca.2013.03.032.

References

[1] K.E. Toghill, R.G. Compton, Int. J. Electrochem. Sci. 5 (2010) 1301.
[2] R. Chawla, Practical Clinical Biochemistry: Method and Interpretations, 3rd ed., Jiltendar P Vij, New Delhi, 2003.
[3] C.H. Walker, J.V.St. John, P. Wisian-Neilson, J. Am. Chem. Soc. 123 (2001) 3847.
[4] B. Wiley, T. Herricks, Y. Sun, Y. Xia, Nano Lett. 4 (2004) 1739.
[5] S. Iijima, Nature 354 (1991) 58.
[6] M. Nath, C.N.R. Rao, J. Am. Chem. Soc. 123 (2001) 4842.
[7] H. Qiu, J. Zhai, S. Li, L. Jiang, M. Wan, Adv. Funct. Mater. 13 (2003) 928.
[8] E.C. Walter, M.P. Zach, F. Favier, B.J. Murray, K. Inazu, J.C. Hemminger, R.M. Penner, Chem. Phys. Chem. 4 (2003) 138.
[9] L. Liang, J. Liu, C.F. Windisch, G.J. Exarhas Jr., Y. Lin, Angew. Chem. Int. Ed. 41 (2002) 3668.
[10] A. Safavi, F. Farjami, Biosens. Bioelectron. 26 (2011) 2552.
[11] Y. Fang, Y. Ni, G. Zhang, C. Mao, X. Huang, J. Shen, Bioelectrochemistry 88 (2012) 7.
[12] B. Unnikrishnan, S. Palanisamy, S.M. Chen, Biosens. Bioelectron. 39 (2013) 75.
[13] S. Wu, G. Liu, P. Li, H. Liu, H. Xu, Biosens. Bioelectron. 38 (2012) 294.
[14] C. Zhou, Y. Shi, X. Ding, M. Li, J. Luo, Z. Lu, D. Xiao, Anal. Chem. 85 (2013) 1176.
[15] W. Jia, W. Liu, Y. Zhang, M. Cui, S. Shuang, C. Dong, M.M.F. Choi, Anal. Methods 4 (2012) 1437.
[16] B.W. Park, R. Zheng, K.A. Ko, B.D. Cameron, D.Y. Yoon, D.S. Kim, Biosens. Bioelectron. 38 (2012) 301.
[17] X. Hu, J. Ji, Langmuir 26 (2009) 2629.
[18] Q. Meng, D. Chen, L. Yue, J. Fang, H. Zhao, L. Wang, Macromol. Chem. Phys. 208 (2007) 484.
[19] D.I. Gittins, F. Caruso, Angew. Chem. Int. Ed. 40 (2001) 3004.
[20] M. Brust, D. Bethell, D.J. Schiffrin, C.J. Kiely, Adv. Mater. 7 (1995) 797.
[21] C. Mao, C.X. Liang, Y.Q. Mao, L. Li, X.M. Hou, J. Shen, Colloids Surf. B 74 (2009) 365.
[22] C. Mao, L.C. Jiang, W.P. Luo, H.K. Liu, J.C. Bao, X.H. Huang, J. Shen, Macromolecules 42 (2009) 9368.
[23] H. Hu, X.B. Wang, S.L. Xu, W.T. Yang, F.J. Xu, J. Shen, C. Mao, J. Mater. Chem. 22 (2012) 15369.
[24] R.K. Kainthan, S.R. Hester, E. Levin, D.V. Devine, D.E. Brooks, Biomaterials 28 (2007) 4590.
[25] R.K. Kainthan, M. Gnanamani, M. Ganguli, T. Ghosh, D.E. Brooks, S. Maiti, J.N. Kizhakkedathu, Biomaterials 27 (2006) 5390.
[26] D.B. Sacks, D.E. Bruns, D.E. Goldstein, N.K. Maclaren, J.M. McDonald, M. Parrott, Clin. Chem. 48 (2002) 472.
[27] S. Suganuma, K. Nakajima, M. Kitano, D. Yamaguchi, H. Kato, S. Hayashi, J. Am. Chem. Soc. 130 (2008) 12793.
[28] X. Wu, P. Du, P. Wu, C. Cai, Electrochim. Acta 54 (2008) 743.
[29] G. Zoldák, A. Zubrik, A. Musatov, M. Stupák, E. Sedlák, J. Biol. Chem. 279 (2004) 47609.
[30] X. Ren, D. Chen, X. Meng, F. Tang, X. Hou, D. Han, L. Zhang, J. Colloid Interface Sci. 334 (2009) 187.
[31] S. Bharathi, M. Nogami, S. Ikeda, Langmuir 17 (2001) 4.
[32] J. Jia, B. Wang, A. Wu, G. Cheng, Z. Li, S. Dong, Anal. Chem. 74 (2002) 2223.
[33] R. Liang, J. Qiu, P. Cai, Anal. Chim. Acta 534 (2005) 229.
[34] M. Şenel, C. Nergiz, Curr. Appl. Phys. 12 (2012) 1124.
[35] D. Feng, F. Wang, Z. Chen, Sens. Actuators B: Chem. 138 (2009) 544.
[36] M. Zhou, L. Shang, B. Li, L. Huang, S.J. Dong, Biosens. Bioelectron. 24 (2008) 447.
[37] X.H. Kang, J. Wang, H. Wu, I.A. Aksay, J. Liu, Y.H. Lin, Biosens. Bioelectron. 25 (2009) 905.
[38] C.S. Shan, H.F. Yang, D.X. Han, Q.X. Zhang, A. Ivaska, L. Niu, Biosens. Bioelectron. 25 (2010) 1074.
[39] H. Zheng, H. Xue, Y. Zhang, Z. Shen, Biosens. Bioelectron. 17 (2002) 545.